euspen's 18th International Conference & Exhibition, Venice, IT, June 2018
www.euspen.eu

Numerical simulation of extrusion-based additive manufacturing – effect of the nozzle geometry on the strand cross-section

Raphaël Comminal[1], Marcin P. Serdeczny[1], David B. Pedersen[1], Jon Spangenberg[1]

[1] *Department of Mechanical Engineering, Technical University of Denmark, Kgs. Lyngby, Denmark*

rcom@mek.dtu.dk

Abstract
The shape of the printed strand in extrusion-based additive manufacturing is an important factor that affects the surface roughness and the geometrical accuracy of the 3D printing fabrication. We used Computational Fluid Dynamics simulations to investigate the effect of the geometry of the extrusion nozzle on the cross-section of the printed strand. The extrusion of a single thread on a planar surface was modelled as an isothermal incompressible Newtonian fluid flow. The deposition of the strand is a creeping flow that solely depends on the geometry of the nozzle, the gap and the ratio of the extrusion speed to the printing speed. We considered three different nozzle geometries: a cylindrical nozzle, a square nozzle, and a cylindrical nozzle with a side plate extension retaining side flows. The numerical simulations provided the cross-section of the deposited strand as well as the printing force applied by the extruded material on the substrate. The side plate improved the compactness of the strand cross-section, while the square nozzle did not present any advantage as compared to the cylindrical nozzle, in the printed configuration that we considered.

3D printing; Extrusion; Flow; Simulation

1. Introduction

The cross-section of deposited strands in extrusion-based additive manufacturing affects the geometrical accuracy and the surface roughness of the fabricated part [1, 2]. In the literature, it is typically assumed that the layer thickness is equal to the gap between the extruder and the substrate. Then, the width of the deposited thread is simply calculated by mass conservation, assuming an idealised strand cross-section, which is either elliptic, oblong, or rectangular.

In a previous study [3], we showed with *Computational Fluid Dynamics* (CFD) simulations of the extrusion flow that the cross-section of the deposited strand can vary from being almost cylindrical to a flat cuboid with rounded edges, depending on the gap between the printing head and the substrate and the printing speed. A reduction of the gap or an increase in printing speed enhances the side flow of the extruded material, causing more elongated cuboid shapes. In contract, an increase of the gap or a faster printing promotes more circular strands. However, strands with circular cross-sections results in a higher porosity of the fabricated part, which negatively affects its mechanical properties [2, 4]. Nevertheless, it was also found that the extrusion of more compact strands with almost cuboid cross-sections requires a larger printing force, which is not desirable either, as it may cause printing instabilities [5].

In the present work, we use CFD simulations to investigate the effect of the geometry of the extrusion nozzle on the shape of the deposited strand. Our aim is to enhance the compactness of the strands (with more cuboid cross-sections), while keeping low printing forces. We consider two alternative geometries of the extrusion nozzle: first an extrusion nozzle with a square cross-section, and secondly a cylindrical nozzle with a side plate extension material (like in Contour Crafting [6]) retaining the side flow. The strand deposition flows of these nozzles are also compared to those of the conventional cylindrical nozzle.

2. Numerical model

2.1. Problem specification

We consider the deposition of a single thread on a planar surface. The geometry of the simulation consists in a static extrusion nozzle, positioned with a gap g above a planar surface. The table moves with a constant tangential velocity V. The three nozzle geometries that we considered are: (i) a cylindrical nozzle with diameter D, (ii) a square nozzle with side width D, and (iii) the cylindrical nozzle with a side plate orthogonal to the table and parallel to the printing direction.

Only half of the geometry is included in the simulation, whenever possible, by virtue of symmetry. An inlet boundary with a uniform velocity U is specified at the entry of the nozzle. The uniform velocity profile shortly rearranges inside the nozzle into a fully-developed laminar flow. All the other boundaries of the geometry are either solid walls (the nozzle wall and the moving table), or outlet boundary conditions (on the side of the calculation domain). The dimensions of the geometry are set long enough such that the position of the boundary conditions does not affect the results of the simulation.

2.2. Physical assumptions

The flow is governed by the conservation of mass and momentum. The extruded material is modelled as an incompressible Newtonian fluid. As a first approximation, we consider that the material properties (density ρ and viscosity μ) are independent of the variations of temperature between the nozzle and the table. Hence, the extrusion is simulated as an isothermal flow.

Moreover, both the inertial effect and the gravity force are negligible (although included in the simulations). Therefore, the extrusion of the material is a creeping flow that is solely determined by the geometry and the boundary conditions of the model. Hence, the predictions of the simulations apply to any

molten material having a kinematic viscosity $\nu = \mu/\rho$ large enough such that $\nu \gtrsim 10\,UD$, which is the case of most thermoplastics used for 3D printers. Thus, the extrusion flow is parametrized by the normalized gap g/D and the printing speed ratio V/U.

We refer the readers to Ref. [3] for more details about the numerical model and the governing equations.

2.3. Numerical methods

The CFD simulations of the strand deposition are performed with the software ANSYS® Fluent R15.0. The governing equations of the flow are discretized in term of flux balances inside control volumes, with the finite volume method. The velocity and pressure fields are solved implicitly, with a fully coupled approach. The free-surface of the extruded material is tracked with the coupled level-set/volume-of-fluid method. The temporal evolution of the system is solved incrementally, with a resolution of $\delta t = 0.01$ s, until the flow reaches a steady state. The maximum size of the control volumes is $\delta l = 0.06$ mm.

3. Results

The CFD simulations provide the entire velocity and pressure fields of the extrusion flows. The cross-section of the deposited strand are measured far away from the printing head, where the strand has reached a steady shape and moves uniformly with the substrate. Figure 1 represents three-dimensional views of the extruded material with a cross-sectional cut of the strand, obtained with the different nozzle geometries, for the printing configuration where $g/D = 1.2$ and $V/U = 0.5$. As the square nozzle has a larger throughput than the cylindrical nozzle, we also simulated the case of the square nozzle with a higher printing speed, where $V/U = 0.75$ (Figure 1c). Table 1 reports the compactness of the cross-section, defined as the ratio of the area of the cross-section by the product of its maximum width and thickness, as well as the printing forces applied on the substrate by the extruded material.

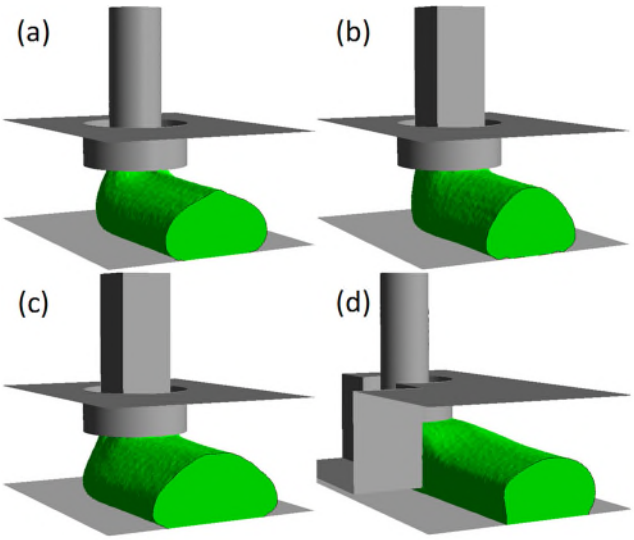

Figure 1. Three-dimensional representations of the extruded material with a cross-sectional cut of the strand, for different nozzles geometries: (a) cylindrical nozzle with $V/U = 0.5$, (b) square nozzle with $V/U = 0.5$, (c) square nozzle with $V/U = 0.75$, and (d) cylindrical nozzle with the side plate extension. In the four snapshots, the gap is $g/D = 1.2$.

First, we observe that the square nozzle does not produce more cuboid cross-sections of the deposited strand, while it requires a larger printing force than the cylindrical nozzle, in the same printing configuration. Secondly, we can see that the addition of the side plate to the cylindrical nozzle enhances the compactness of the cross-section by restraining the side flows below the printing head. The presence of the side plate increases the printing force, but it remains lower than for the square nozzle.

Table 1. Compactness of the strand cross-sections and printing forces, for the different printing configurations.

Printing configurations with $g/D = 1.2$	**Cross-section compactness**	**Printing force/N**
Cylindrical nozzle with $V/U = 0.50$	0.770	0.039
Square nozzle with $V/U = 0.50$	0.773	0.055
Square nozzle with $V/U = 0.75$	0.751	0.034
Cylindrical nozzle plus side plane with $V/U = 0.5$	0.854	0.048

4. Conclusions

The extrusion of a molten material and its deposition on a planar surface have been simulated with a CFD model. As a first approximation, the molten material is modelled as an isothermal incompressible Newtonian fluid. The deposition flow is entirely determined by the geometry and the boundary conditions of the model, as the extrusion is a creeping flow.

The preliminary results show that the square nozzle does not improve the compactness of the deposited strand, and increases the printing force on the substrate, in the printing conditions that we considered. In contrast, the extrusion with the cylindrical nozzle plus a side plate enhances the compactness of the strand cross-section by retaining the side flow, while it increases moderately the printing force.

Future works should investigate other printing configurations, with different gaps and printing speed ratios. The numerical simulation could also be used to find the optimal dimensions and position of the side plate.

References

[1] Turner B N and Gold S A 2015 *Rapid Prototyp. J.* **21** 250-61.
[2] Mohamed O A, Masood S H and Bhowmik J L 2015 *Adv. Manuf.* **3** 42-53.
[3] Comminal R, Serdeczny M P, Pedersen D B and Spangenberg J 2018 *Addit. Manuf.* **20** 68-76.
[4] Rodríguez J F, Thomas J P and Renaud J E 2003 *Rapid Prototyp. J.* **9** 219-30.
[5] Turner B N, Strong R and Gold S A 2014 *Rapid Prototyp. J.* **20** 192-204.
[6] Khoshnevis B, Bukkapatnam S, Kwon H and Saito J 2001 *Rapid Prototyp. J.* **7** 32-42.